Available online at www.sciencedirect.com
SCIENCE DIRECT
Mechatronics 16 (2006) 249–257
MECHATRONICS

Force display using a hybrid haptic device composed of motors and brakes

Tae-Bum Kwon, Jae-Bok Song *

Department of Mechanical Engineering, Korea University, 5, Anam-Dong, Seongbuk-Gu, Seoul 136-713, South Korea

Received 19 April 2005; accepted 21 December 2005

Abstract

In the virtual environment, force feedback to the human operator makes virtual experiences more realistic. However, the force feedback using active actuators such as motors can make the system active and sometimes unstable. To ensure the safe operation and enhance the haptic feeling, system stability should be guaranteed. Both active actuators such as motors and passive ones such as brakes are commonly used for haptic devices. Motors can generate a torque in any direction, but they can make the system active and thus, sometimes unstable during operation. On the other hand, brakes can generate a torque only against their rotation, but they dissipate energy during operation and this dissipation makes the system intrinsically stable. Consequently, motors and brakes are complementary to each other. In this research, a two degree-of-freedom (DOF) haptic device equipped with motors and brakes is designed, in which each DOF is actuated by a pair of motor and brake. Simultaneous operation of motors and brakes is analyzed. Models for some environments, virtual wall contact and frictional effect, are proposed. The results for the hybrid haptic system are compared with those for the active haptic system and the passivity based control system. The experimental results show that the hybrid haptic device is more suited to some applications than the other haptic systems.

Keywords: Hybrid haptic devices; FME; Virtual wall contact; Frictional effect

1. Introduction

Among the human's five senses, visual and auditory senses have been widely exploited in the field of human–computer interaction. The other senses are usually much more difficult to display in the virtual environment. A haptic device is the mechanical interface used to display force or tactile sense when a human interacts with the virtual environment or the remote system. Haptic devices vary in size and type, from small devices for tactile display of the fingertip to very large devices for displaying whole body motion.

Most haptic devices employ motors or brakes as a main power source to generate haptic effects. A motor as an active actuator can generate a desired torque in any direction at a relatively fast speed. But the force feedback may make the haptic system active and sometimes unstable, which significantly degrades a user's feeling [1]. In contrast, a brake is always stable because it only dissipates energy and is capable of generating a larger torque per unit mass than a motor. Furthermore, it consumes relatively small amount of energy consumption, making it suitable for portable devices. Since most real or virtual environments can be modeled as passive systems, use of passive actuators such as brakes for haptic devices can be justified. However, a brake can generate a torque only against the direction of its motion or only against an externally applied torque [2]. This feature may be beneficial from the stability point of view, but it often leads to poor performance in passive haptic devices because they are not able to generate a torque in an arbitrary direction. Another drawback of a brake is its relatively slow response, which makes it difficult to display the haptic effects that require fast responses.

* Corresponding author. Tel.: +82 2 3290 3363; fax: +82 2 3290 3757.
E-mail address: jbsong@korea.ac.kr (J.-B. Song).

0957-4158/$ - see front matter © 2006 Elsevier Ltd. All rights reserved.
doi:10.1016/j.mechatronics.2005.12.003

Most haptic devices have been designed with one type of actuator and mostly motors are preferred. In the motor-based haptic systems, good haptic performance can be easily achieved, but it is hard to ensure the stable operation under a wide variety of operating conditions, especially when a large contact force with the virtual wall is represented. Several algorithms have been proposed to guarantee the stability of the haptic interfaces. Adams was able to derive optimal virtual coupling parameters with the dynamic model of a haptic device by using the two-port network theory [3]. This virtual coupling provided a fixed amount of damping, and thus sometimes degraded the realistic feeling because of excessive dissipation of energy. The new energy-based schemes such PO/PC (passivity observer/passivity controller) and the energy bounding algorithm were proposed by Hannaford and Ryu [4,5]. These methods measured and controlled the amount of energy that flowed in and out of the system to satisfy the passivity condition. But the sampling rate of the system should be sufficiently greater than the system modes to stabilize the system with this scheme. The energy bounding algorithm required good estimation of the damping coefficients in the physical haptic devices. Even if these conditions were satisfied, realistic feeling of the haptic interface could be degraded when the contact with the stiff virtual wall took place.

In the brake-based passive haptic systems, stability of the system can be guaranteed, but the haptic performance is relatively poor, so most research has focused on their performance improvement. Swanson developed the haptic device equipped with brakes and clutches and controlled it using the concept of the velocity field to perform the arbitrary path following [6]. The simulation and experimental results were good, but the device was not very practical because only the experiments involving small contact forces and velocities were presented. In [2], a two-link manipulator equipped with only brakes was developed. With the concept of force manipulability ellipsoid, the region available for force reflection could be determined. But it was not practical because successful haptic display at one instant could not guarantee successful path guidance along the virtual path.

Since motors and brakes are complementary to each other in various respects, use of both a motor and a brake may lead to better haptic effects. Such a device was presented in [7]. A 3 DOF force output device equipped with motors and magnetic particle brakes was presented by using a two-axis gimbal linkage and translating central shaft. Advantages and disadvantages of a combined brake and motor were also discussed. In this research a 2 DOF hybrid haptic device equipped with two types of actuators serially connected to a common axis will be presented. This device can be activated in three modes; a motor-only mode, a motor-and-brake mode, and a brake-only mode. However, a pure passive haptic device composed of only brakes has difficulties in displaying various haptic effects, and thus, it will be excluded in this research. This research is aimed at comparing the active haptic system, where only motors are used for force display, with the hybrid haptic system where both motors and brakes are involved in force display. Among many types of force displays, this research has focused on the cases with very large contact force (e.g., greater than 100 N) and frictional effects. It will be shown that the proposed hybrid haptic system is more suitable to these cases than the conventional active haptic systems. For example, haptic devices used for virtual sports like boxing should handle from a small force to a very large force. In this application, a hybrid haptic system can stably generate a wide range of forces. In addition, some effects related to friction such as a sawing task are more stably and realistically represented by the proposed hybrid haptic system composed of brakes and motors.

The remainder of this paper is organized as follows: Section 2 presents the design procedure and the structure of the 2 DOF hybrid haptic device, which will be used as the main experimental setup for this research. Section 3 describes the control of the proposed hybrid haptic device, and Sections 4 and 5 describe the display methods for the virtual wall contact and frictional surface experimentally. Finally, Section 6 presents the conclusions.

2. Design of a hybrid haptic device

2.1. Linkage mechanism and workspace

As shown in Fig. 1, a 2 DOF haptic device was developed based on the 5-bar linkage. Among the five joints, J_1 and J_2 are the actuated joints, while the others are passive. The active joints are serially connected to both the motors and the brakes to form a *hybrid* device. In addition, they are also connected to the optical encoders from which

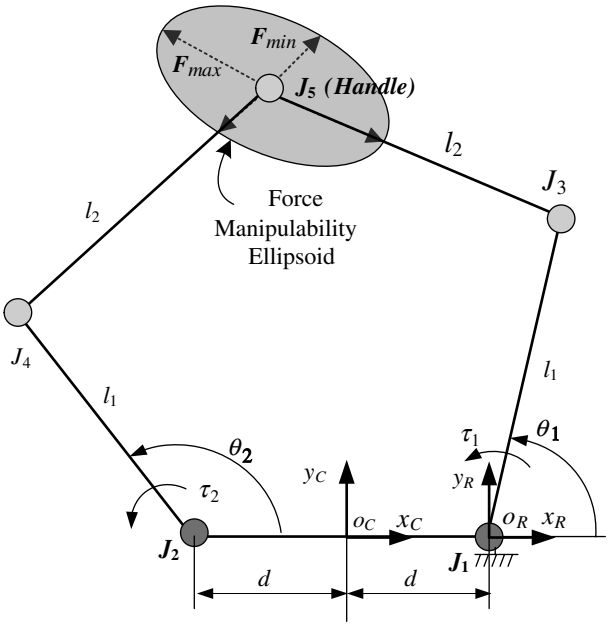

Fig. 1. Linkage mechanism for 2 DOF haptic device.

the end-effector position can be computed by the Jacobian relation. The shape and size of the workspace of the end-effector is determined by the length of each link (l_1, l_2), the distance between two active joints $(2d)$, and the allowable rotational ranges of the active joints. From the simulation results for various parameters, the lengths of all links were chosen as 200 mm, the distance between two active joints as 0 mm, the rotational ranges of J_1 and J_2 as $-40°$ to 110° and 70–220°, respectively. With these parameters, the workspace was generated in the range of -190 mm to 190 mm in the x-axis and 90 mm–320 mm in the y-axis, as shown in Fig. 2 (i.e., 380 mm × 230 mm). The device can generate a desired force in any direction within the workspace since no singularity exists.

2.2. Selection of power and actuator output

The first step in designing a haptic device is the determination of its output. According to the quantitative analysis of the force that an average person can generate instantaneously [8], the device should exert a force more than 80 N. Considering this factor, the haptic device was designed to produce the maximum force of more than 80 N in all directions over the whole workspace.

The maximum force that the device can produce varies depending on the configuration of the linkage and the direction of the force exerted by the linkage. To analyze this force generation, the concept of FME (force manipulability ellipsoid) was adopted [2]. The relationship between the joint torque vector τ and the end-effector force vector F is given by

$$\tau = J(q)^{\mathrm{T}} \cdot F \tag{1}$$

where J is the Jacobian matrix dependent on the configuration of the joint angles $q = \{\theta_1\, \theta_2\}^{\mathrm{T}}$ of the active joints. The end-effector force can then be computed by

$$F = [J(q)^{\mathrm{T}}]^{-1} \cdot \tau \tag{2}$$

The FME is the trajectory of the force in the Cartesian space when the joint torque is constrained to $\|\tau\| = 1$. This FME can be easily found by varying the angle ϕ in $\tau = [\cos\phi\ \sin\phi]^{\mathrm{T}}$ in the range of 0–2π. Fig. 2 shows the FME simulation results for the force generated by the motor output in the designed workspace. Since the minimum forces for all configurations shown in the figure are greater than 80 N, the motor-driven device can create a force greater than 80 N in all directions of the whole workspace. The Maxon 120W BLDC motor along with the speed reducer was used to generate a torque of 4.44 N m. This output torque was further amplified by a set of pulleys with the 5:1 ratio, thus generating the designed force at the end-effector.

For the passive part of the device, the Ogura particle brake OPB-40N was selected. The maximum torque of this brake was 4 N m, and about 0.08 N m was needed to rotate the axis for no load condition. One drawback of the brakes was its time constant of 50 ms which was much slower than that of the motor, 7 ms. The response time of the brake is important because some haptic effects require collision during a short interval. The other characteristics such as hysteresis of a brake were referred to [7]. It was found from the FME simulations that the brake-driven device could passively exert a force greater than 36 N in all directions in the whole workspace.

2.3. System structure

Fig. 3 shows the photo of HHD (hybrid haptic device) constructed for this research, and Fig. 4 shows the schematic diagram of HHD. Pulley 1 is connected to both motor 1 and brake 1 through the flexible coupling on the identical axis, and the torque generated by the motor and/or brake is delivered from pulley 1 to pulley 3 through the tendon-driven mechanism. The axis of pulley 3 coincides with joint 1, from which two links 1 and 3 are serially

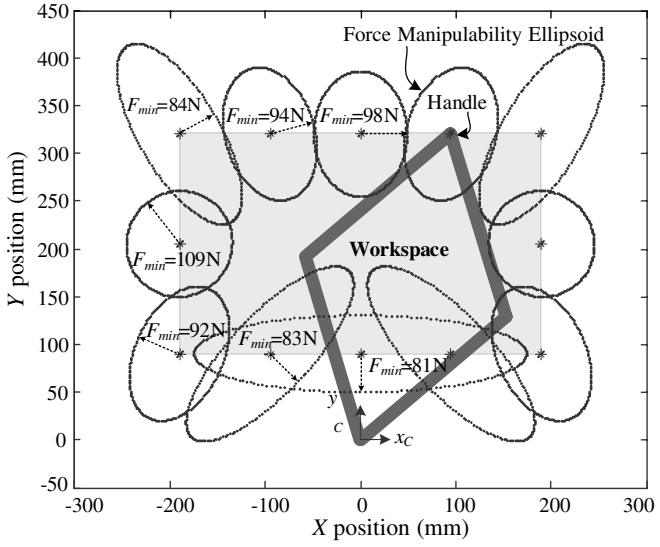

Fig. 2. FME simulation results for motor-driven device in whole workspace.

Fig. 3. Photo of hybrid haptic device.

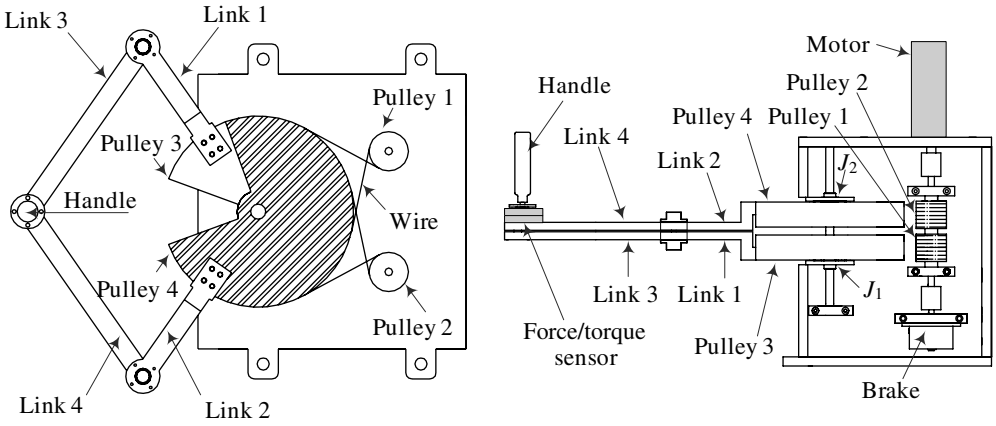

Fig. 4. Basic structure of hybrid haptic device.

connected. On the other hand, by the same mechanism, the torque is delivered to pulleys 2 and 4. The axis of pulley 4 coincides with joint 2, from which two links 2 and 4 are serially connected. Since link 0 between J_1 and J_2 has a zero length, the 5-bar linkage with link 0 and links 1–4 can be formed as shown in Fig. 4. The force that a user exerts or feels is measured by the force/torque sensor installed at the end-effector of HHD.

3. Control of a hybrid haptic device

It is generally difficult to use a brake in the haptic device because a passive actuator cannot generate a torque in an arbitrary direction but only against the direction of its rotation. A promising use of brakes is to dissipate a large amount of energy as proposed in [7]. In this hybrid motor and brake control scheme, the system monitored the power requirement of the virtual environment and activated the brakes whenever dissipative elements were simulated. The feedback force provided to the user was accomplished by the motor output alone according to the virtual model.

A similar approach will be adopted in this research. As an example, the virtual wall compression is considered here. Suppose the virtual wall modeled as a spring is displayed with one axis controlled by a motor and the other by a brake as shown in Fig. 5. When the virtual wall is compressed by the end-effector as shown in Fig. 5(a), the motor force F_{m} and the brake force F_{b} result in a resultant force F_{r} perpendicular to the virtual wall. This is possible because the brake force is opposite to the motion of the end-effector and thus, the inner product of the motion vector and the brake force vector becomes negative in the xy plane.

But when the reaction force of the virtual wall is larger than the force exerted by the human operator and the end-effector is released as shown in Fig. 5(b), the resultant force of the motor force and the brake force is not perpendicular to the virtual wall. This is because the brake can exert only a reaction force against its outward motion, which is $F_{\mathrm{b.actual}}$. Since the force generated by the device is not $F_{\mathrm{r.desired}}$, which is perpendicular to the virtual wall but $F_{\mathrm{r,actual}}$, the generated motion is not perpendicular to the virtual wall. Although it is easy to understand this behavior in joint space, the behavior in Cartesian space is given in Fig. 5 because the actual contact with the virtual wall occurs in this space.

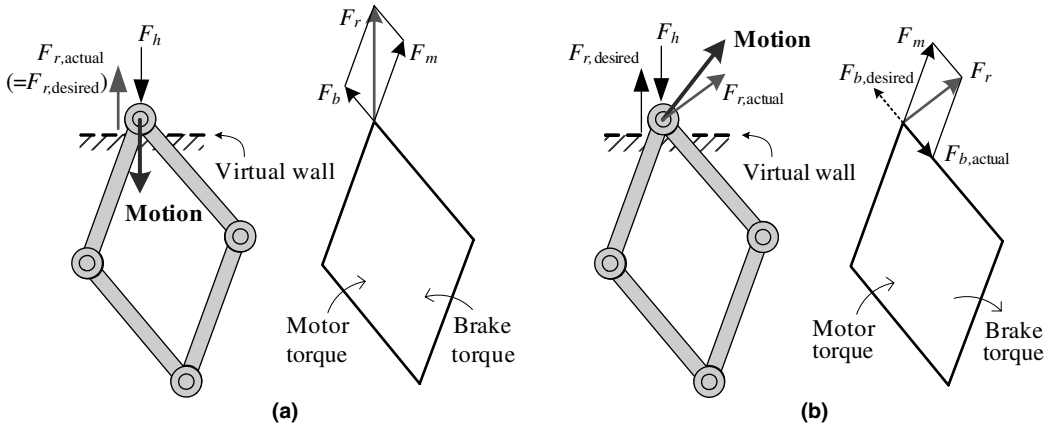

Fig. 5. Control of hybrid system: (a) compression of virtual wall and (b) release of virtual wall.

Therefore, it is natural that the motion direction and the force applied by the user are considered as an input to the brake control algorithm. If the desired direction of a force measured by the force/torque sensor is opposite to the motion direction computed by the encoder, the brake can apply the force in the proper direction. In many haptic effects, the device exerts forces in the direction opposite to the motion. Thus, motors and brakes can be used simultaneously when the force is desired in the direction opposite to the motion; otherwise, only motors can be used.

4. Representation of virtual wall contact

One of the most important haptic effects is contact with a virtual wall. Due to time delay and limitation of the actuators, contact with the virtual wall displayed by the haptic device is somewhat different from real contact. Moreover, the system can become unstable depending on the control method and the experimental conditions. It is important, therefore, for the haptic systems to remain stable during haptic display.

Generally, a virtual wall can be displayed by using one kind of actuators, motors or brakes. When only brakes are used to display the virtual wall and the end-effector penetrates it, the brakes are activated to prevent the end-effector from moving further into the virtual wall. If the response of the brake is fast enough to stop the end-effector the instant it penetrates the wall, one can experience the realistic touch with the wall. Moreover, the system always remains stable since brakes are passive at all times. However, since the response of a brake is generally slow, the end-effector can be stopped only after penetration occurs to some extent. In addition, the passive haptic device using brakes cannot exert the forces that push the end-effector out of the virtual wall surface because the brake can only generate a reaction force against the force exerted by a human operator. The brakes used in the hybrid haptic device have relatively long response time, so contact with the virtual wall was not well represented.

When only motors are used to represent haptic effects, the virtual wall is usually modeled as a spring-damper system, and the main force is computed by multiplying the penetration depth by the spring stiffness. As the penetration depth increases, the reaction force from the motor also increases. When this force becomes larger than the hand force applied by the operator, the end-effector moves back to the surface of the virtual wall, and the operator feels contact with the virtual wall. Since the response time of the motor is relatively faster than that of the brake, the operator can experience a more realistic contact feeling. However, if the virtual wall is assumed to have high stiffness, the reaction force from the motor may be excessively large, which tends to destabilize the system (e.g., persistent vibration). Even a big bounce can take place at the initial contact, especially when the contact velocity is high or the contact force is large.

The motor-based haptic system can display the virtual wall based on a damper model instead of a spring model. In this case, the reaction force is a function of the end-effector velocity. Thus the reaction force is large at the initial contact with the virtual wall due to the high velocity, but it continues to decrease as the penetration proceeds. The human operator can feel a crisp force upon initial contact because a large force is generated at contact. But after the velocity is reduced by the reaction force, the end-effector penetrates into the virtual wall continuously because the reaction force is relatively small. Rosenberg studied the human operator's feeling about the virtual wall modeled as a spring and that modeled as a damper using statistical tools [9]. But this research had limitations in that the maximum motion range was small and the stiffness of the virtual wall used in the experiment was just 7 N/mm.

In this research, a new method for representing more realistic haptic effects by using a hybrid haptic system is presented. The system is equipped with both motors and brakes. Contact with the virtual wall occurs at a velocity faster than 1 m/s and with a force greater than 100 N. Fig. 6(a) is a virtual wall model which consists of a spring, a damper and a brake, and Fig. 6(b) represents the ideal relationship of force versus position during wall contact. If the wall stiffness is very high, the wall is little compressed when subjected to the force. For the hybrid haptic system equipped with both motors and brakes, a damper model is more suitable than a spring model. The instant the contact with the virtual wall occurs, the brakes are activated and the motors generate the damping force as a function of the end-effector velocity. The slow response of the brakes can be compensated by the motors whose response is relatively fast. Therefore, before the brake output takes effect at initial contact, a large damping force proportional to the velocity is generated by the motor. The damping force generated by the motor reduces as the velocity decreases, whereas the brake output replaces the motor output to control the end-effector position.

If the damper is assumed to be linear, a large force cannot be generated at the initial contact. If a large damping coefficient is chosen to compensate for this lack of force, a large force can be generated at the initial contact, but

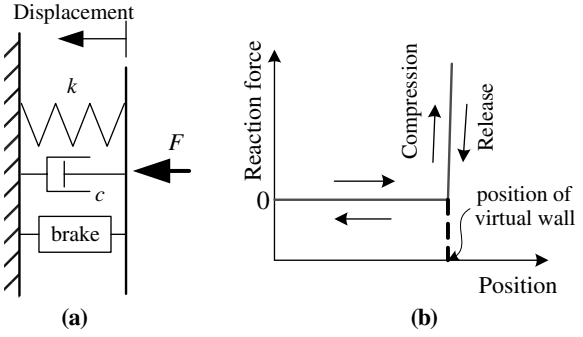

Fig. 6. Virtual wall model and ideal relation of force versus position during contact with stiff wall.

the force remains large at all times, which leads to possible instability of the system. To cope with this problem, a nonlinear damper was designed so that its output at high velocities becomes much larger than that of a linear damper.

In the real experiments, the unstable condition was observed in the velocity range of 20–40 mm/s when the damper model with large coefficients was employed. The output of HHD differed depending on the linkage configuration, but it could generate the force more than 80 N in the whole workspace and 100 N in a major portion of the workspace. Therefore, as shown in Fig. 7, the coefficient was designed so that the force of 100 N would be generated above the velocity of 40 mm/s and decreased suddenly below it. If the desired force is greater than the actuator limits, the output force is saturated to the maximum force. In this research, the damper model of $F = 1{,}600{,}000 * v^3$ (F: N, v: m/s) was adopted.

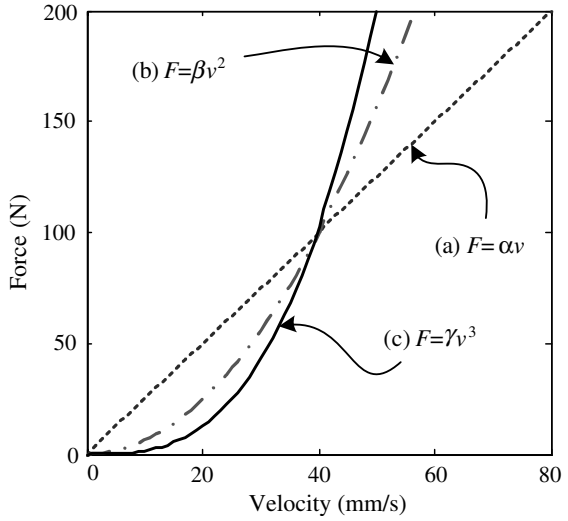

Fig. 7. Different dampers used in experiments: (a) linear damper, (b) and (c) nonlinear dampers.

In Fig. 8 the pure active haptic system and the active haptic system based on the PO/PC scheme were compared with the hybrid haptic system using both motors and brakes. In both the pure active system and the PO/PC-based system, the wall was modeled as a spring with stiffness of 150 N/mm, whereas in the hybrid system, it was modeled as a nonlinear damper model $F = 1{,}600{,}000 * v^3$. Fig. 8 shows the experimental results for weak contact when the contact velocity was about 250 mm/s and the human operator felt a force of 20–30 N. For the pure active system, bounces occurred during the transient period of 0.11 s, but the steady-state error was very small. For the PO/PC based system, only one bounce occurred at the initial contact and a small steady-state error existed. This response was similar to that of the pure active system but more stable. For the hybrid system, the transient period was about 0.11 s, but no bounce was observed. A large steady-state error of 1.2 mm occurred and at the instant

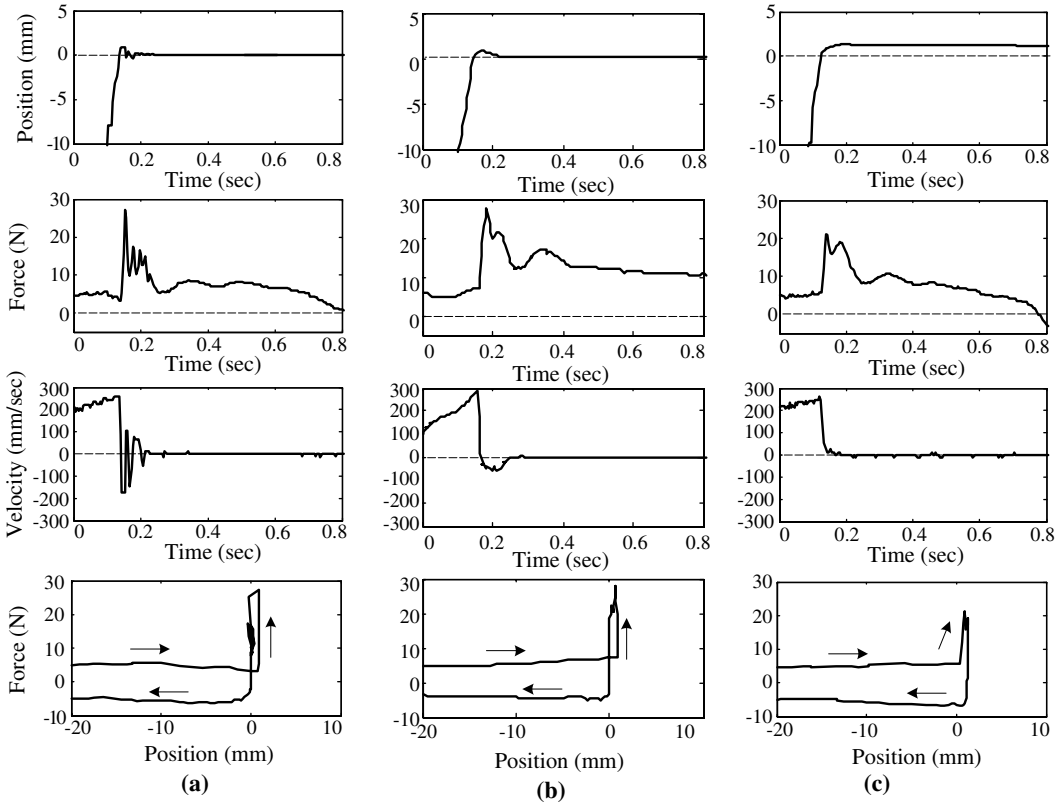

Fig. 8. Experimental results for contact with hard wall at low velocities: (a) active haptic system, (b) PO/PC based haptic system, and (c) hybrid haptic system.

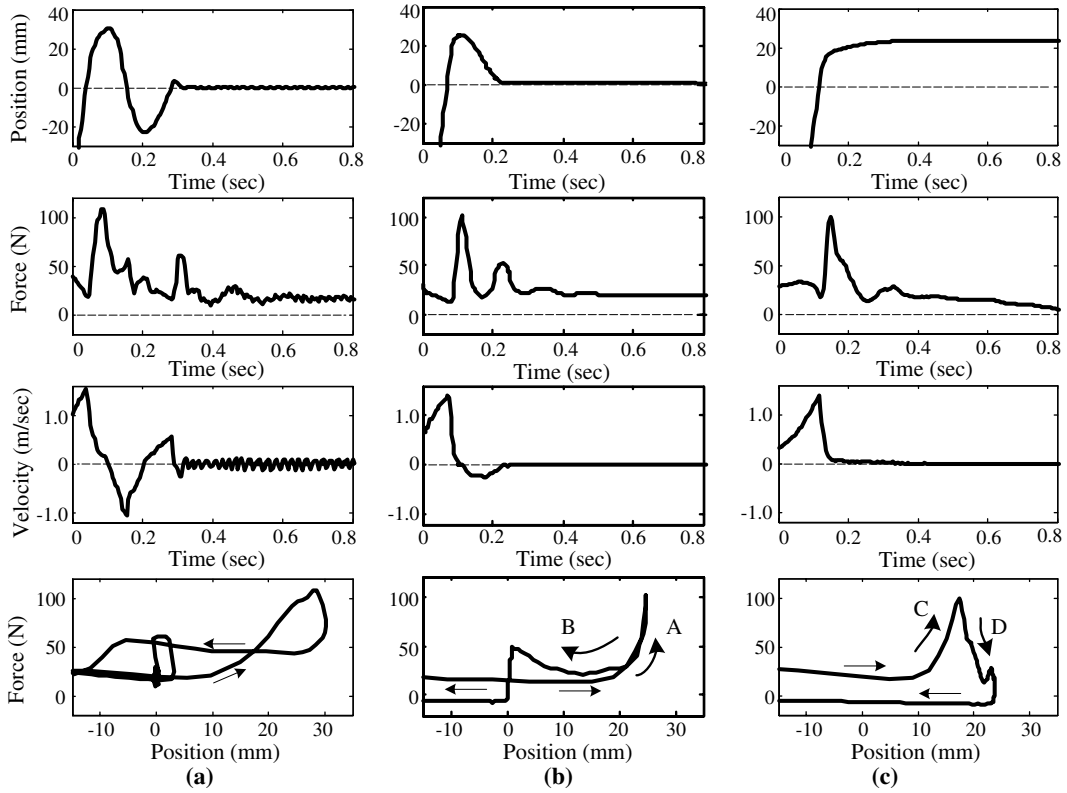

Fig. 9. Experimental results for contact with hard wall at high velocities: (a) active haptic system, (b) PO/PC based haptic system, and (c) hybrid haptic system.

of 0.12 s the end-effector velocity dropped sharply. The three plots showing the force versus the position in Fig. 8 were similar to that of Fig. 6(b), thus meaning that these three systems well represented contact with the hard wall at low velocities. Note that the time span of the graphs of position (force, velocity) versus time is 0.8 s, whereas that of the graph of force versus displacement is much longer than 0.8 s. This graph was sketched to show approach to the wall, compression of the wall, release of the wall, and departure from the wall in a row.

Fig. 9 shows the experimental results for strong contact when the contact velocity was as high as 1500 mm/s and the human operator experienced a contact force over 100 N. The pure active system suffered unstable oscillation and big bounces, while the PO/PC based system showed one big bounce and then stable response. A small steady-state error was observed in both systems. On the other hand, the hybrid system did not exhibit any bounce and remained stable after contact with the wall, but the steady-state error was very large up to about 20 mm, because deep penetration arose due to the high velocity before the brake was really activated. In this case, the accurate position of the virtual wall could not be represented.

Although the hybrid system showed an overshoot which caused a large steady-state error, it could be beneficial in the light of a user's contact feeling. In the pure active system and the PO/PC based system, the big bounce in position generated kind of a pushing force by which the user experienced that the end-effector of the device was suddenly pushed away from the wall immediately after the wall deformation, which was unlikely to occur in the real wall contact. This could be observed in the graph of the force versus position of Fig. 9(b), in which the user felt a hard initial contact force labeled A, but immediately underwent a pushing force labeled B that was caused by the virtual spring model. In the hybrid system, however, the user

Table 1
Comparison of three haptic systems for contact with hard virtual wall

	Active haptic system	PO/PC based haptic system	Hybrid haptic system
Wall model	Only spring	Spring + adjustable damper	Damper + brake
Advantage	Small steady-state error	Small steady-state error	Similar to ideal relation of force versus position at wall contact Realistic feeling for contact at high velocities
Disadvantage	Unstable oscillation	Less realistic feeling for contact at high velocities	Large steady-state error

could experience a braking force by which the end-effector suddenly stopped after contact. As can be seen in the graph of the force versus position of Fig. 9(c), the user felt a hard initial contact force labeled C and then a braking force labeled D exerted by the real brake. This behavior is close to the ideal behavior shown in Fig. 6(b), except for a steady-state error. Consequently, as far as the realistic feeling is concerned, the response of the hybrid system is better than those of the other systems. The wall models, advantages and disadvantages of the three haptic systems discussed above are summarized in Table 1.

5. Representation of frictional surface

As shown in Fig. 10(a), friction arises when two objects slide in contact with each other. This friction can be divided into static and dynamic friction. To represent the friction effect using HHD, the human operator pushes the virtual object in contact with the virtual frictional surface. The force normal to the frictional surface was measured by the force/torque sensor, and it was multiplied by the friction coefficient to compute the friction force. Two different cases were tested. In the first case, both the friction force and the reaction force (i.e., normal force) of the virtual wall were displayed by the motor output, whereas in the second case, the friction force was displayed by the brake output and the reaction force by the motor output. The ideal relationship between the external force and the friction force relationship is shown in Fig. 10(b).

The force F_{hy}, the y component of the hand force F_h, was measured by the force–torque sensor and was multiplied by the friction coefficient μ to yield the friction force F_f. If the motors are used to display the friction force and this computed friction force is greater than the x component F_{hx} of the hand force, then the active motion against the hand force is generated by the friction force, which cannot occur physically. Thus, the friction force was carefully restricted to less than or equal to F_{hx} to prevent the active motion from occurring. When the brakes are used, the friction force is computed by multiplying the normal force by the friction coefficient without any concern about the active motion because the brake forces are always passive. However, since the brake force is limited in its direction, brakes should be controlled depending on the direction of the force exerted by the human operator.

The friction display based on the active system was compared with that of the hybrid system. In the hybrid system, the friction force was generated by the brakes but the normal force by the motors. The stability and performance of the hybrid system were investigated when the end-effector moved on the virtual surface while being depressed. Fig. 11 shows the experimental result for the weak normal force under 25 N. In both systems, the computed forces were a little different from the measured ones because of the friction of the mechanism. But careful observation of the measured force and the x displacement in Fig. 10(b) showed that the static friction force increased gradually, decreased suddenly, and converted into the dynamic fric-

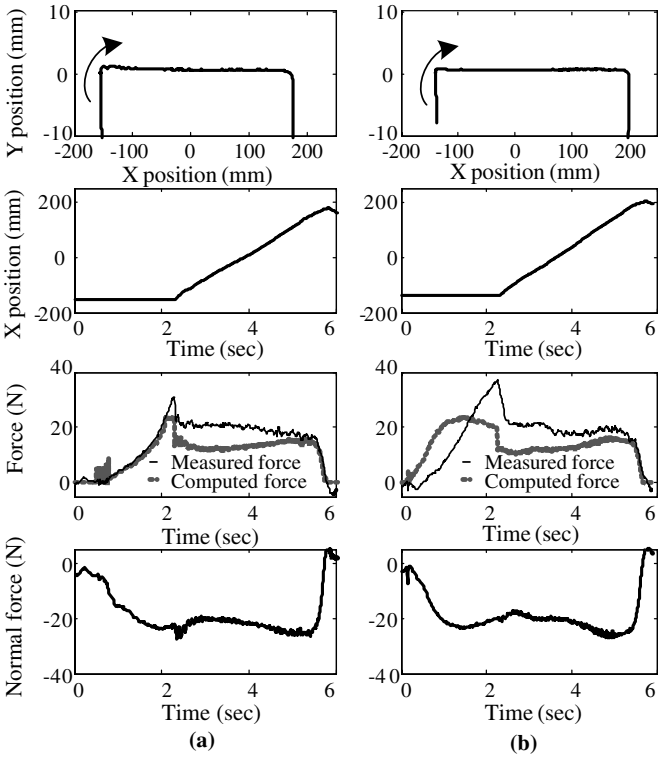

Fig. 11. Results for friction experiment with small normal force: (a) active haptic system and (b) hybrid haptic system.

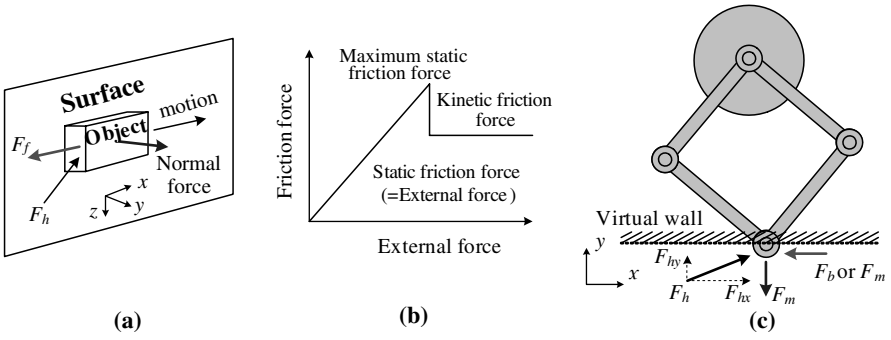

Fig. 10. Representation of friction effect: (a) friction model, (b) relationship between external force and friction force, and (c) forces acting on the system to represent friction.

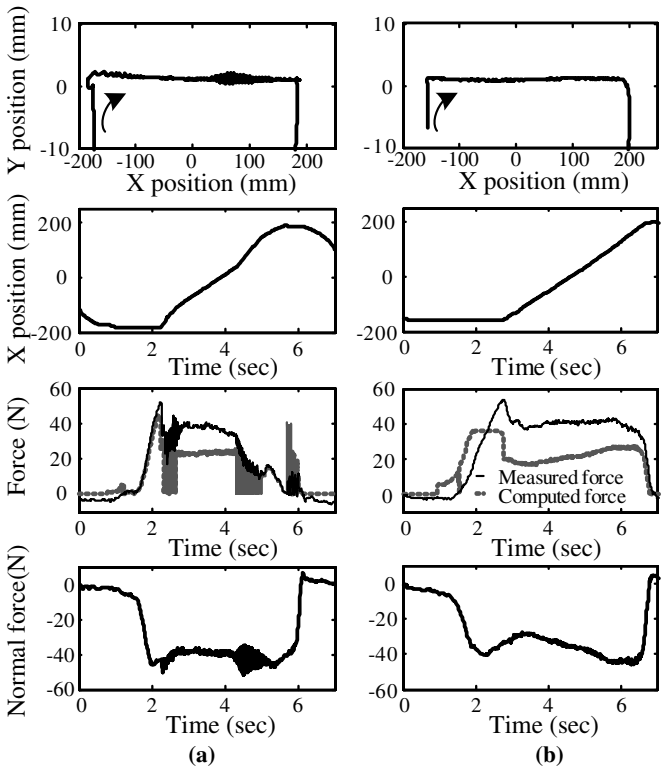

Fig. 12. Results for friction experiment with large normal force: (a) active haptic system and (b) hybrid haptic system.

tion force. Fig. 12 shows the experimental result when a large normal force over 40 N was imposed. The active system was more likely to become unstable because both normal and friction forces were displayed by the active motors, as shown in Fig. 12(a).

In summary, in displaying the friction effects, the hybrid system is better suited to some situations (e.g., pushing the object on the wall or sawing) than the active system, in which a large normal force can produce an undesired frictional force.

6. Conclusions

In this research, a new type of hybrid haptic system was designed to take advantages of both active and passive actuators serially connected to a common axis. The hybrid haptic system was compared with the active haptic device in terms of stability and performance when displaying the virtual wall contact and the friction effects. Its responses were also compared with those of the PO/PC based haptic system when displaying the virtual wall contact which is one of the most important haptic effects.

If contact with the stiff virtual wall is displayed by the active system using only motors, the steady-state error of the end-effector position can be small after contact, but the system itself may be unstable. Although the PO/PC based haptic system can shows good performance in various situations, it tends to generate a big bounce during high velocity contact with the stiff virtual wall, which causes the user to feel a less realistic pushing force. When the hybrid haptic system is used, it always remains stable and the user feels a realistic braking force during contact with the stiff virtual wall, but a large steady-state error occurs due to the nature of a brake. It is desirable, therefore, that the hybrid system should be employed when the realistic feeling of contact with the stiff wall (for example, a punch of a boxer) is to be displayed. In the display of the friction effects, the force normal to the frictional surface exerted by the human operator always varied, and so did the friction force. Therefore, the hybrid system is better suited to some situations (e.g., sawing) than the active system.

Although the active haptic systems or the PO/PC based haptic systems are generally better than the hybrid haptic system, the latter can sometimes give better results in some situations, especially, for case of strong contact with the virtual wall or frictional effects. The researches on the hybrid system control for more various haptic effects are under way.

Acknowledgement

This work was supported by grant no. (R01-2003-000-10336-0) from the Basic Research Program of the Korea Science & Engineering Foundation.

References

[1] Colgate JE, Grafing PE, Stanley MC, Schenkel G. Implementation of stiff virtual walls in force-reflecting interfaces. In: Proceedings of IEEE virtual reality annual international symposium, 1993. p. 202–8.
[2] Cho CH, Kim MS, Song JB. Performance analysis of a 2-link haptic device with electric brakes. In: Proceedings of IEEE international symposium on haptic interfaces and tele-operator systems, 2003. p. 47–53.
[3] Adams RJ. Stable haptic interaction with virtual environments. Doctor's dissertation, Washington University, 1999.
[4] Hannaford B, Ryu JH. Time-domain passivity control of haptic interfaces. IEEE Trans Robot Autom 2002;18(1):1–10.
[5] Kim JP, Ryu JH. Stable haptic interaction control using energy bounding algorithm. In: Proceedings of IEEE international conference on intelligent robots and systems, 2004. p. 1210–7.
[6] Swanson DK, Book WJ. Path-following control for dissipative passive haptic displays. In: Proceedings of IEEE international symposium on haptic interfaces and tele-operator systems, 2003. p. 101–8.
[7] Russo M, Tadros A. Controlling dissipative magnetic particle brakes in force reflective devices. In: Proceedings of advances in robotics, ASME, dynamic systems and control division, vol. 42; 1992. p. 63–70.
[8] Tan H, Srivasan M, Eberman B, Cheng B. Human factors for the design of force-reflection haptic interfaces. In: Proceedings of ASME winter annual meeting, DSC-vol. 55-1; 1994. p. 353–9.
[9] Rosenberg LB, Adelstein BD. Perceptual decomposition of virtual haptic surfaces. In: Proceedings of IEEE VR annual international symposium, 1993. p. 46–53.